RESEARCH

Open Access

Mediastinal lymphadenopathy in sarcoidosis: Can diffusion MRI play a role in its evaluation?

Youssriah Yahia Sabri[1], Naglaa Mahmoud Mohamed Mahmoud[1], Mohammed Raafat Abd El–Mageed[1], Marwa Mohammed Mohammed Onsy[1], Sabah Ahmed Mohamed[2], Mahmoud Mohamed Mohamed Onsy[3,4] and Mostafa Ahmed Khairy[1]*

Abstract

Background Sarcoidosis is a multisystem disease defined by non-caseous epithelioid cell granulomas that can affect virtually all organs. Lung, mediastinal and hilar lymph node involvement is prevalent, occurring in around 90% of the patients, and is responsible for the majority of the morbidity and mortality related to the disorder. Sarcoidosis is one of the differential diagnoses of the benign mediastinal lymphadenopathy. This research aimed to detect the diagnostic value of magnetic resonance imaging (MRI) diffusion in evaluation of mediastinal lymphadenopathy in sarcoid patients.

Results This cross study involved a total of 30 patients known to have sarcoidosis: 6 males and 24 females aged between 18 and 50 years (with a mean age 38.97 ± 8.67); all of them presented with mediastinal lymphadenopathy. For all patients, each lymph node group was evaluated for the average size and average ADC value. The mean ADC measured was $(1.76 \pm 0.28) \times 10^{-3}$ mm^2/s. Eight patients showed concurrent activity with poor response to the treatment, and they showed different ADC values with one of them showing low ADC with pattern of diffusion restriction displaying mean ADC value of 1.28×10^{-3} mm^2/s.

Conclusions Diffusion-weighted MRI is an established imaging technique that could be utilized to evaluate mediastinal lymphadenopathy in sarcoidosis as the benign counterpart of mediastinal lymphadenopathy.

Keywords Sarcoidosis, Mediastinal lymphadenopathy, MRI diffusion, ADC value

*Correspondence:
Mostafa Ahmed Khairy
Mostafakhairy11@gmail.com
[1] Department of Diagnostic and Interventional Radiology, Kasr Al Ainy Faculty of Medicine - Cairo University, Giza, Egypt
[2] Chest Department, Kasr Al Ainy, Faculty of Medicine - Cairo University, Giza, Egypt
[3] World Health Organization Egypt Office, Cairo, Egypt
[4] Global Health and Development, Hanyang University, Seoul, South Korea

Background

Sarcoidosis is a multisystem granulomatous disease with unclear origin and a broad range of clinical and imaging symptoms [1]. It affects typically young and middle-aged adults, with the frequency peaking in the third decade of life. In the majority of research, females have higher incidence rate than males [2, 3].

The lung and the intra-thoracic lymph nodes are the most affected organs; both occur in over than 90% of cases [2, 3]. Sarcoidosis can appear with a variety of radiologic patterns; the most prevalent are interstitial lung disease and bilateral hilar lymph node enlargement [1].

Sabri *et al. Egypt J Radiol Nucl Med*   (2023) 54:60

Page 2 of 9

Approximately 95% of individuals with sarcoidosis present with enlargement of bilateral hilar and right paratracheal lymph nodes [2]. In less than 5% of patients, isolated unilateral enlargement of the hilar lymph node (often on the right side) is spotted. It is much less frequent to find mediastinal lymph node enlargement without hilar lymph node affection [4].

Eventually, the swollen nodes may calcify. As with other chronic granulomatous diseases, the incidence of lymph node calcification in sarcoidosis is directly proportional to disease duration; calcification develops within 5 years in 3% of patients and within 10 years in 20%. Calcifications may appear punctuated, amorphous, popcorn-like, or eggshell-like [2].

CT imaging is the primary radiological investigation method. It depends on many factors such as lymph node location, size, and distribution. Sarcoidosis cases with atypical features might imitate malignancy on CT scans [4, 5].

PET/CT is a validated imaging method for mediastinal lymphadenopathy evaluation as it combines the functional information of PET with the comprehensive anatomical data of CT in a single examination [6]. Nevertheless, sarcoidosis can still become a problem in PET CT scanning and might even result in false positive results of malignancy since the lymph nodes in sarcoidosis may have increased FDG uptake just like those of malignancy [7].

Magnetic resonance imaging (MRI) is becoming a helpful imaging technique for the mediastinum, in addition to digital radiography and computed tomography [8]. MRI is preferable to these techniques because it does not expose patients to radiation and can offer greater soft tissue characterization. Diffusion-weighted magnetic resonance imaging (DWI) visualizes the microscopic movement and diffusion of water molecules in tissues, which is strongly impacted by the intracellular organelles, cellular water content and macromolecules. Therefore, DWI gives useful information for a functional assessment of tissue microstructure in respect to anatomy and is utilized to differentiate lymphadenopathy as benign or malignant [9].

In our study, we were aiming to detect the diagnostic value of MRI diffusion in evaluation of mediastinal lymphadenopathy in sarcoidosis patients.

Methods
Study design
Retrospective cross-sectional study including 30 patients known with sarcoidosis: 6 males and 24 females aged between 18 and 50 years (mean age of 39).

This study was conducted after institutional and departmental ethical clearance over a period of 20-month duration (starting from January 2021 till August 2022). The range of symptoms included chest discomfort, dyspnea and cough.

Inclusion criteria
Patients diagnosed with sarcoidosis by computed tomography and histopathology.

Exclusion criteria
Contraindications for MRI, such as cochlear implant, pacemaker, ocular metallic foreign body, cerebral aneurysm clips and bullet or gunshot near major blood arteries or important organs.

MRI technique
All patients underwent MRI of the mediastinum using a 1.5 T unit (Achieva; Philips Medical Systems).

Image acquisition
Conventional MRI images
A 16-channel phased array torso coil (Sense XL Torso; Philips Healthcare) was utilized to obtain axial T1 WI, axial and coronal T2 WI images. Respiratory gating was used.

MR imaging parameters:

- Initially, three plane localizers were acquired to localize and design the sequences utilizing rapid single-shot localizers.
- We acquired T1WI using a spin echo sequence in the subsequent specifications: number of excitations: 2; echo time/repetition time: 5 ms/10 ms; section thickness: 8 mm; direction of frequency encoding: R/L; field of view: 36–40 cm; gap: 0.5 mm; matrix: 288×224.
- We acquired T2WI using a spin echo sequence in the subsequent specifications: echo time/repetition time, 80 ms/664 ms; direction of frequency encoding: R/L; number of excitations, 3; gap, 1.5 mm; section thickness, 8 mm; matrix, 288×224; field of view, 36–40 cm.

Diffusion-weighted magnetic resonance imaging images (DWI)

- Diffusion-weighted images were obtained for all the examined cases using the following parameters:
- Typically, DWI is obtained in a transverse plane, utilizing these three b values; high b value (1000 s/ mm^2), intermediate (500 s/ mm^2) and low (0–50 s/ mm^2). The usual thickness of the slice is between 4 and 9 mm, the interslice gap is between 0 and

Sabri *et al. Egypt J Radiol Nucl Med* (2023) 54:60

Page 3 of 9

1.5 mm, and the number of excitations spans from 1 to 10.

- The apparent diffusion coefficient (ADC) maps were computed by the MR system utilizing linear regression analysis of the natural log of signal intensity with each of the three b values (0, 500 and 1000 s/mm^2).

Image evaluation

The images are interpreted by three cardiothoracic radiologists having 11 to 25 years of expertise. After a debate between the two readers, their disagreement was settled by consensus (consensus decision) after a discussion with a third radiologist having over 25 years of expertise.

MR images were subjected to both qualitative & quantitative examination of the various pulse sequences.

a. Qualitative (visual) assessment

Each group of lymph nodes was evaluated for size, and signal intensity relative to that of muscles in the pulse sequences T1 WI, T2 WI as well as its signal in DWI and ADC map.

On DWI and ADC maps, lymph nodes were evaluated qualitatively by comparing their signal strength on the high-*b*-value (*b* = 1000 s/mm^2) DWI to that on the matching ADC map.

Associated MR imaging findings, e.g., pleural or pericardial effusions, and upper abdominal lesions were recorded.

b. Quantitative assessment

Minimum and mean ADC values shown in units of $\times 10^{-3}$ mm^2/s were calculated for all mediastinal and hilar lymph nodes detected.

Values of ADC were obtained using ADC maps created using $b = 0$, $b = 500$, and $b = 1000$ s/mm^2 values. A central region of interest (ROI) was defined, and the size of the ROI was maintained as broad as feasible on the ADC map in order to prevent macroscopic necrosis and major blood vessels with conventional imaging. The final result was reported as the average of three measurements. In the assessment of lymph nodes, only lymph nodes with size more than 1 cm were measured for ADC value.

Statistical methods and data analysis

Statistical analysis was performed using SPSS version 26 for Windows to code and enter data (IBM Corp., Armonk, NY, USA). Quantitative data were summarized using measures of mean, standard deviation, median, minimum, and maximum, while frequency (count) and relative frequency were used to summarize the qualitative data (%). Analyzing quantitative data required the use of the non-parametric Mann–Whitney test. Chi-square

Table 1 Lymph node distribution in the sarcoid patients

Lymph node group	Patient count	%
RT paratracheal lymph nodes	30	100
Hilar lymph nodes	30	100
Subcarinal lymph nodes	28	93.3
Prevascular lymph nodes	6	20.0
Para esophageal lymph nodes	2	6.7
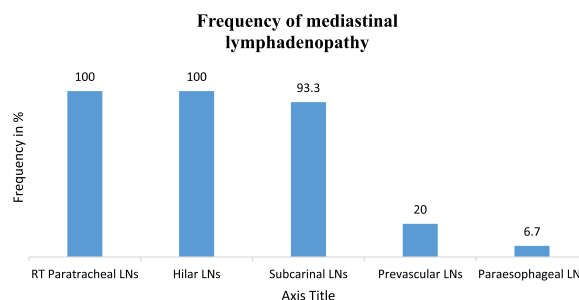
Fig. 1 Distribution of the lymph nodes in the sarcoid patients

analysis was used to compare groups of nominal variables. An exact test was utilized when the expected frequency was under 5. Relationships between numerical variables were studied using Spearman's correlation coefficient [10].

Results

This cross study involved a total of 30 patients known to have sarcoidosis: 6 males and 24 females aged between 18 and 50 years (with a mean age 38.97 ± 8.67). They presented by various symptoms as dyspnea, cough and chest pain.

They all presented with mediastinal lymphadenopathy. Lymph nodes were identified and localized as follows: right paratracheal (in 30 patients), hilar (in 30 patients), subcarinal (in 28 patients), prevascular (in 6 patients), para esophageal posterior meditational (in 2 patients) (Table 1) (Fig. 1).

On conventional MR images, all lymph nodes displayed intermediate T1 WI signal. On T2 WIs, 22 cases displayed intermediate signal, 7 cases displayed high T2 signal and 1 case displayed dark signal.

For all patients, each lymph node group was evaluated for the average size as shown in (Table 2). Dimensions (short axis) of the lymph nodes ranged between 1.1 and 4 cm (median dimension = 1.8 cm).

Qualitative assessment of DWI and ADC map

Lymph nodes in patients with sarcoidosis showed faint high signal in DWI and variable signal in ADC map (26

Sabri *et al. Egypt J Radiol Nucl Med*   (2023) 54:60

Page 4 of 9

Table 2 Size of the mediastinal lymph nodes in each group

	Mean	Standard deviation	Median	Minimum	Maximum
Prevascular average size (cm)	1.83	0.54	2.10	1.10	2.30
RT paratracheal average size (cm)	1.85	0.41	1.80	1.10	3.00
Hilar average size (cm)	2.30	0.57	2.20	1.40	4.00
Subcarinal average size (cm)	2.27	0.77	1.80	1.50	4.00
Para esophageal average size (cm)	1.55	0.07	1.55	1.50	1.60

cases showed high signal in ADC map, 3 showed mixed signal, and 1 cases showed low signal in ADC map).

Quantitative assessment and ADC analysis

Average ADC value for each lymph node group was measured as shown in Table 3. The mean ADC for sarcoidosis measured was $(1.76 \pm 0.28) \times 10^{-3}$ mm^2/s (Figs. 2, 3, 4).

Eight patients showed concurrent activity with poor response to the treatment. They showed different ADC values with one of them showing low ADC with significant diffusion restriction displaying mean ADC value about 1.28×10^{-3} mm^2/s (Table 4) (Fig. 5).

About 29 (96.7%) patients had parenchymal affection identified in the CT images. Extra thoracic involvement of the sarcoid was seen in 7 (23.3%) patients; 5 of them had hepato-splenomegaly, one patient had enlarged abdominal lymph nodes, and one patient had parotid gland sarcoid involvement. Associated MRI findings included pleural effusion in one case and pericardial effusion in one case.

Discussion

This research involved the assessment of 30 sarcoidosis patients with mediastinal/hilar lymphadenopathy by MRI chest with DWI; six males and 24 females aged between 18 and 50 years (with a mean age 38.97 ± 8.67). This agreed with Sabri et al. (2017), Ley et al. (2016) and Rodríguez et al. (2013) who stated that sarcoidosis was more common in middle-aged females [11–13].

100% of cases showed involvement of the right paratracheal, bilateral hilar and subcarinal lymph node groups. This was consistent with studies conducted by Rodríguez et al. (2013) and Sabri et al. (2017) where they stated that this was considered as the typical lymphadenopathy pattern for sarcoidosis involvement and occurred in about 95% of cases [11, 13].

Sarcoidosis contributes as a part of the differential diagnosis of the benign lymphadenopathy. Gümüştaş et al. recorded that the mean ADC for sarcoidosis was $(2.065 \pm 0.518) \times 10^{-3}$ mm^2/s [9]. Multiple studies were conducted to differentiate the benign from the malignant mediastinal lymphadenopathy using DWI-MRI in cases of sarcoidosis and lymphoma. Sabri et al. reached ADC cutoff value of $(1.525 \times 10^{-3}$ mm^2/s) with sensitivity of 100% and specificity of 100% in the differentiation of lymphoma and sarcoidosis with sarcoidosis showing the higher ADC values [11]. Similarly, Gümüştaş et al. reached the cutoff value of $(1.266 \times 10^{-3}$ mm^2/s); ADC had a sensitivity of 100% and specificity of 81% with sarcoidosis having the higher ADC values [14].

Nearly the same results were encountered by Santos and colleagues in 2021 where the mean ADC was significantly lower in the lymphoma group than in the sarcoidosis group ($0.993 \pm 0.508 \times 10^{-3}$ mm^2/s vs. $1.668 \pm 0.732 \times 10^{-3}$ mm^2/s; $p = 0.002$). The ADC cutoff value that best differentiated between lymphoma-related and sarcoidosis-related enlarged lymph nodes was 1.205, with a sensitivity, specificity, positive predictive value, negative predictive value and accuracy of 87.5%, 82.6%, 85.1%, 84.0% and 86.3%, respectively [15].

Table 3 ADC values for each lymph node group in sarcoid patients

	Mean	Standard deviation	Median	Minimum	Maximum
RT paratracheal average ADC ($\times 10^{-3}$ mm^2/s)	1.70	0.36	1.70	1.10	2.50
Hilar average ADC ($\times 10^{-3}$ mm^2/s)	1.85	0.47	1.80	1.20	3.00
Subcarinal average ADC ($\times 10^{-3}$ mm^2/s)	1.96	0.25	2.00	1.60	2.30
Prevascular average ADC ($\times 10^{-3}$ mm^2/s)	1.8	0.24	1.7	1.60	2.30
Para esophageal average ADC ($\times 10^{-3}$ mm^2/s)	1.50	0.00	1.50	1.50	1.50

Sabri *et al. Egypt J Radiol Nucl Med*   (2023) 54:60

Page 5 of 9
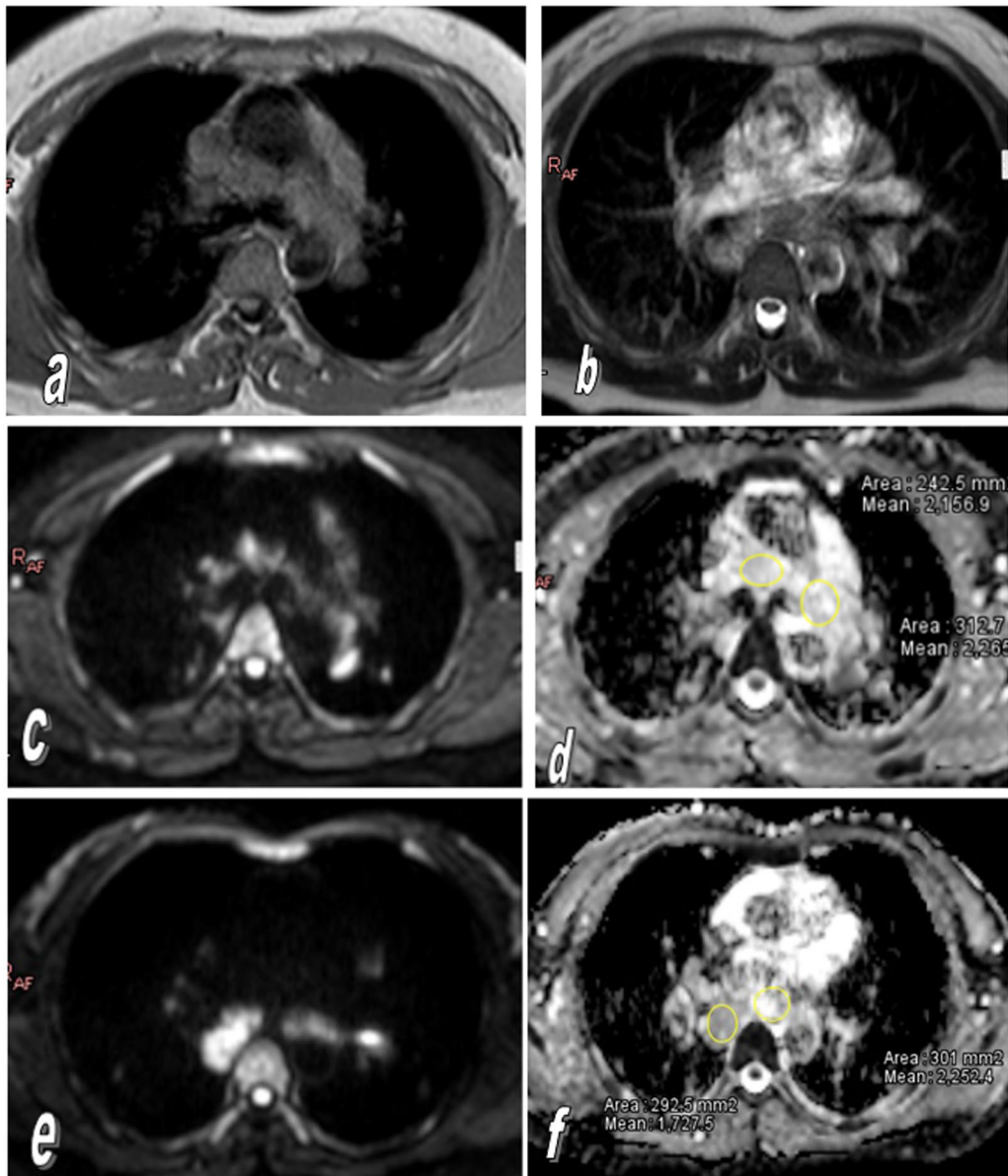
Fig. 2 **a** Axial T1WI, **b** axial T2WI, **c**, **e** diffusion-weighted MRI image, **d**, **f** ADC map showing exuberant partially amalgamated mediastinal lymphadenopathy seen predominantly involving the paratracheal, bilateral hilar and subcarinal lymph node groups as well as prevascular, retrosternal and retrocaval lymph node groups. They display intermediate T1 WI, intermediate to hyperintense T2 WI, hyperintense on DWI and mixed signal on ADC map with mean ADC value of 2.1×10^{-3} mm^2/s

Abdel Razek et al. (2012) reported the lymph nodes' appearance on the DW-MRI and ADC maps. On ADC maps, malignant lymph nodes exhibited low signal intensity, in contrast to the high signal intensity of benign lymph nodes. This was in line with our study where the enlarged lymph nodes were hyperintense on the DW-MRI (100%) and ADC maps (86.6%) [16].

In this research, the mean ADC for sarcoidosis was $(1.76 \pm 0.28) \times 10^{-3}$ mm^2/s, which was consistent with

Sabri et al. (2017) who reported that the mean ADC value of sarcoidosis was $(1.9 \pm 0.28) \times 10^{-3}$ mm^2/s. Almost identical outcomes were observed by Gümüştaş et al. (2013) who showed a mean ADC for sarcoidosis was $(2.065 \pm 0.518) \times 10^{-3}$ mm^2/s [9].

According to Wang et al. (2001), in benign LNs, a misleading reduction in ADC might occur due to the existence of nodal reactive alterations that manifested

Sabri *et al. Egypt J Radiol Nucl Med*   (2023) 54:60

Page 6 of 9
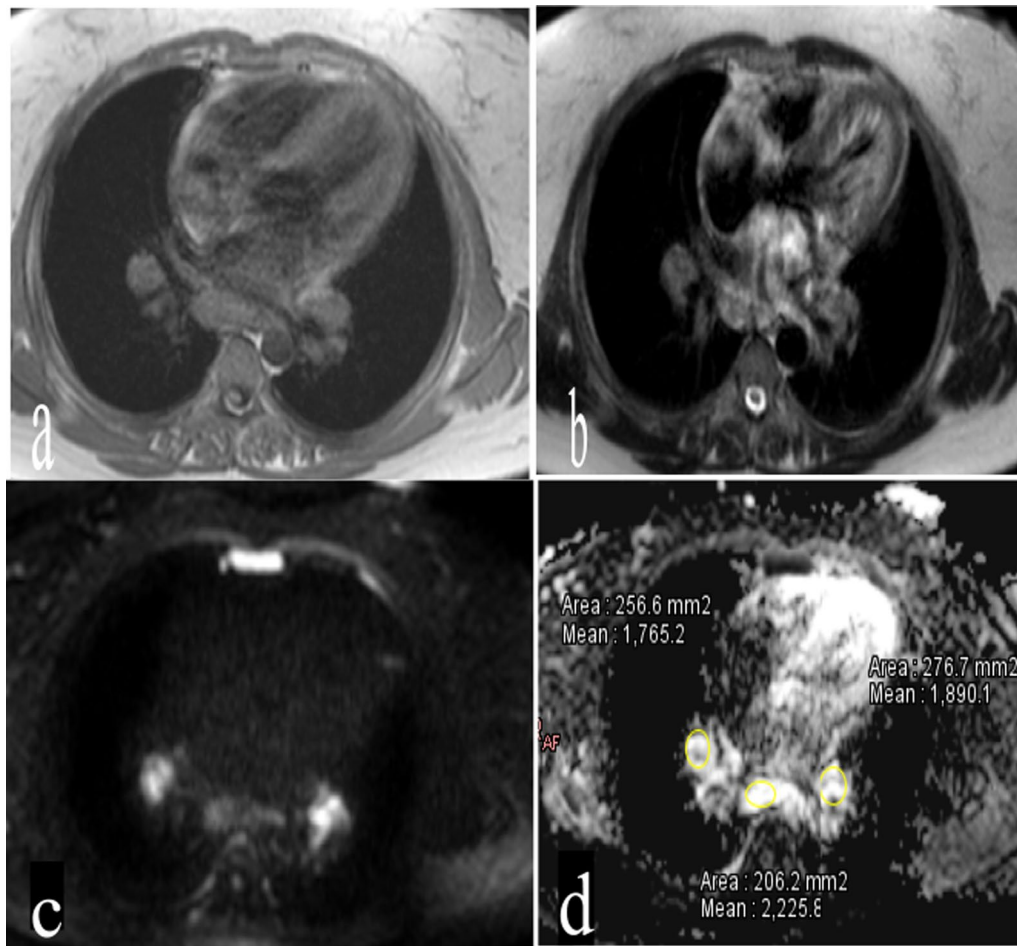
Fig. 3 **a** Axial T1WI, **b** axial T2WI, **c** diffusion-weighted MRI image, **d** ADC map demonstrating bilateral hilar and subcarinal mediastinal lymph nodes that are isointense on T1, hyperintense on T2 WI, and slightly hyperintense on DWI, with a mean value of ADC equal to 1.96×10^{-3} mm^2/s

as fibrotic stroma and numerous germinal centers, which operated as microstructural barriers [17].

This was in line with Abdel Razek et al. (2012) who reported low ADC value in one of their patients with sarcoidosis. Histopathological investigation revealed that dense fibrous reaction with calcification was the predominant reaction in this instance. Different components, including calcification, granulation tissue and fibrous scar tissue, were connected with the limitation of water transport and the resulting decrease in ADC value [16].

In this work, we couldn't establish a solid correlation between sarcoidosis activity and ADC restriction pattern due to limited number of cases with concurrent activity. Thus, further studies with larger sample are recommended to evaluate such correlation.

As with other research, this study had certain limitations. Despite the use of phase array coil with respiratory gating strategies to enhance picture quality, susceptibility artifacts were seen in a few instances. Nonetheless, these artifacts did not compromise the diagnostic information provided by the various MR sequences.

Conclusion

Diffusion-weighted MRI is an established imaging technique that can be utilized to evaluate mediastinal lymphadenopathy in sarcoidosis as they show higher ADC values compared to the previously reported low ADC of malignant thoracic nodes.
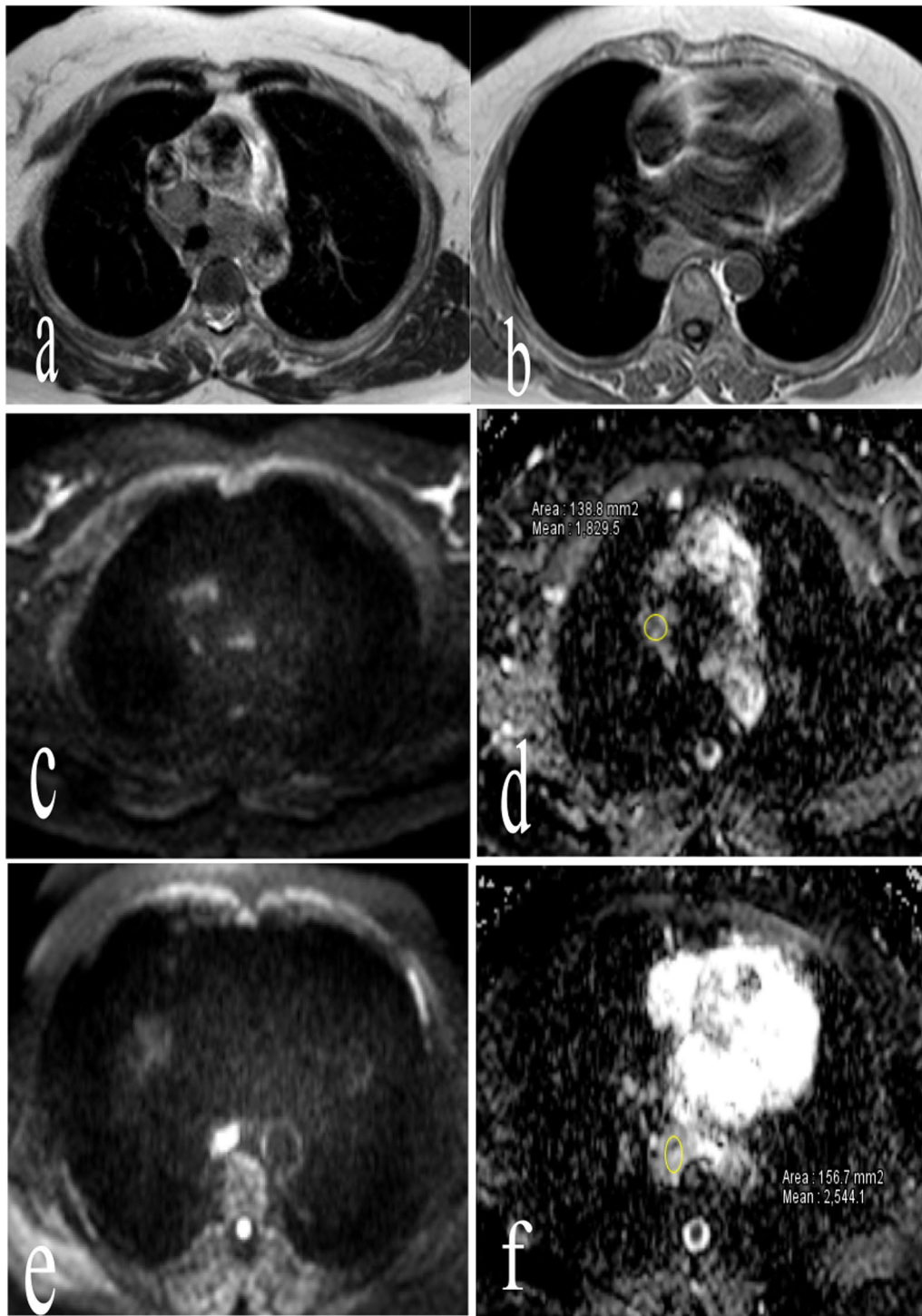
Fig. 4 **a** Axial T2WI, **b** axial T1WI, **c**, **e** diffusion-weighted MRI image, **d**, **f** ADC map showing paratracheal, retrocaval, aortopulmonary, paraesophygeal and small bilateral hilar lymph nodes which are isointense on T1WI, iso to hyperintense on T2 WI, hyperintense on DWI and faintly hyperintense ADC map with mean ADC value of 2.1×10^{-3} mm^2/s

Sabri *et al. Egypt J Radiol Nucl Med*   (2023) 54:60

Page 8 of 9
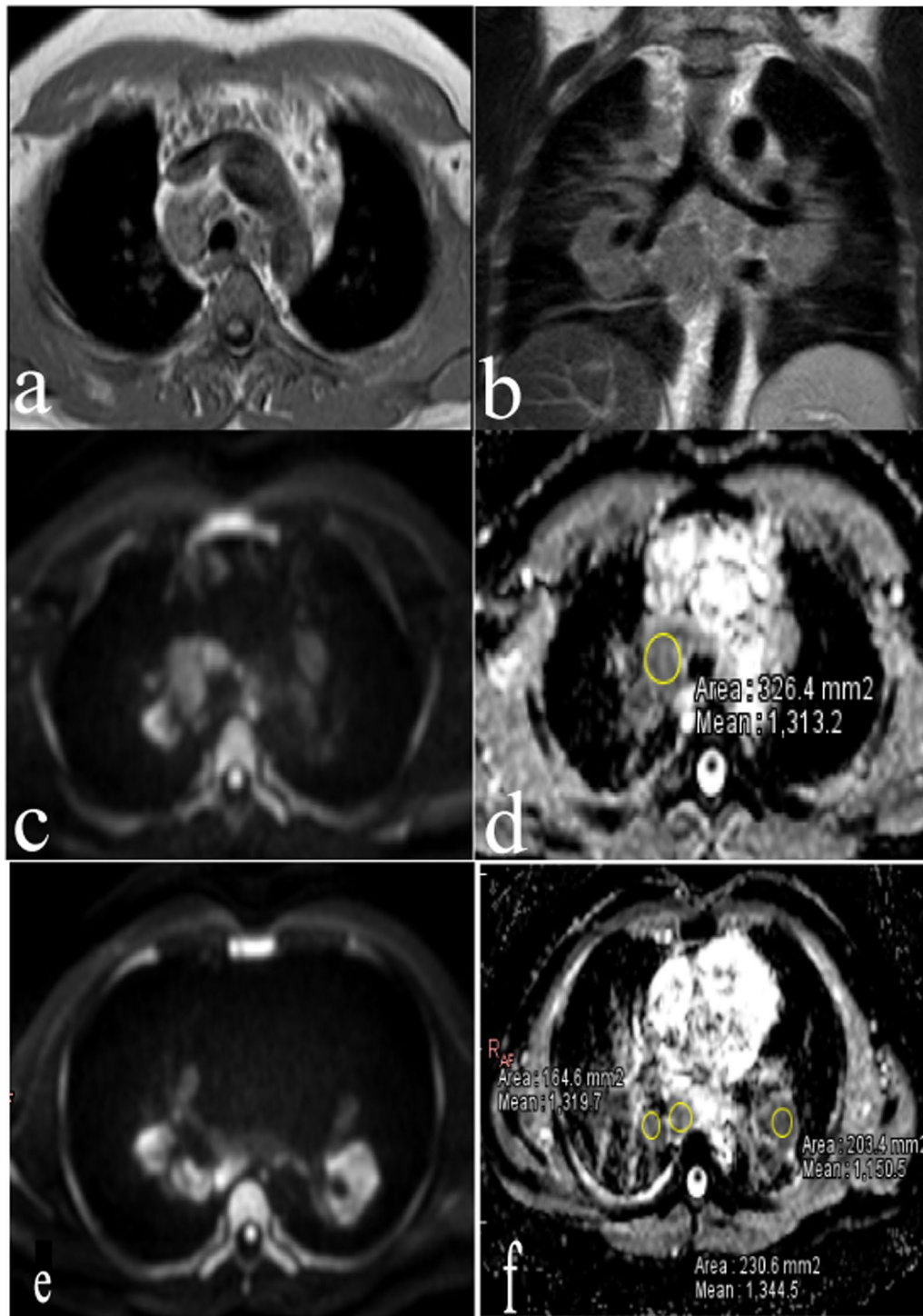
Fig. 5 a Coronal T2WI, **b** axial T1WI, **c**, **e** diffusion-weighted MRI image, **d**, **f** ADC map showing right paratracheal, bilateral hilar, subcarinal and posterior mediastinal lymph nodes which display isointense signal on T1 and hyperintense on T2 WI. They appear faintly hyperintense on DWI with dark signal in ADC map. The mean ADC value is 1.28×10^{-3} mm^2/s

Sabri *et al. Egypt J Radiol Nucl Med*   (2023) 54:60

Page 9 of 9

Table 4 Mean ADC value in the 8 patients with concurrent activity

Patient	Mean ADC ($\times 10^{-3}$ mm^2/s)
No 1	2.1
No 2	1.82
No 3	1.7
No 4	2.2
No 5	1.28
No 6	2.2
No 7	1.9
No 8	2.2

Abbreviations

ADC	Apparent diffusion coefficient
cm	Centimeter
CT	Computed tomography
DWI	Diffusion-weighted images
DLNS	Dark lymph node sign
FDG	Fluorodeoxyglucose
mm^2/s	Square millimeters per second
MRI	Magnetic resonance imaging
PET	Positron emission tomography
ROI	Region of interest
SD	Standard deviation
WI	Weighted images

Availability of data and materials
The datasets used and/or analyzed during the study are available upon reasonable request.

Declarations

Ethics approval and consent to participate
No individual data included in the study. The study was done according to the ethical parameters of all the involved centers and was approved by the Research Ethics Committee of the Faculty of Medicine at Cairo University, reference number not available. All patients included in this study gave verbal informed consent to participate in this research.

Consent for publication
All patients included in this study gave informed consent to publish the data contained within this study.

Competing interests
The authors declare that they have no competing interests.

References
1. Koyama T, Ueda H, Togashi K, Umeoka S, Kataoka M, Nagai S (2004) Radiologic manifestations of sarcoidosis in various organs. Radiographics 24(1):87–104. https://doi.org/10.1148/rg.241035076
2. Criado E, Sánchez M, Ramírez J, Arguis P, de Caralt TM, Perea RJ et al (2010) Pulmonary sarcoidosis: typical and atypical manifestations at high-resolution CT with pathologic correlation. Radiographics 30(6):1567–1586
3. Lee GM, Pope K, Meek L, Chung JH, Hobbs SB, Walker CM (2020) Sarcoidosis: a diagnosis of exclusion. Am J Roentgenol 214:50–58
4. Ganeshan D, Menias CO, Lubner MG, Pickhardt PJ, Sandrasegaran K, Bhalla S (2018) Sarcoidosis from head to toe: what the radiologist needs to know. Radiographics 38(4):1180–1200
5. Hawtin KE, Roddie ME, Mauri FA, Copley SJ (2010) Pulmonary sarcoidosis: the 'Great Pretender.' Clin Radiol 65(8):642–650. https://doi.org/10.1016/j.crad.2010.03.004
6. Mosavi F (2013) Whole-body MRI including diffusion-weighted imaging in oncology. Digital comprehensive summaries of Uppsala dissertations from the Faculty of Medicine. Acta Universitatis Upsaliensis, Uppsala (**ISBN 978-91-554-8796-6**)
7. Shetty A, Carter JD (2011) Sarcoidosis mimicking lymphoma on FDG-PET imaging. Radiol Case Rep 6:409
8. Biederer J, Mirsadraee S, Beer M et al (2012) MRI of the lung-current applications and future perspectives. Insights Imaging 3(4):373–386
9. Gümüştaş S, İnan N, Akansel G et al (1885) Differentiation of lymphoma versus sarcoidosis in the setting of mediastinal–hilar lymphadenopathy: assessment with diffusion-weighted MR imaging. MATTIOLI 2013(30):52–59
10. Chan YH (2003) Biostatistics 102: quantitative data–parametric & non-parametric tests. Singapore Med J 44(8):391–396
11. Sabri YY, Farid Kolta MF, Khairy MA (2017) MR diffusion imaging in mediastinal masses the differentiation between benign and malignant lesions. Egypt J Radiol Nucl Med 48(3):569–580
12. Ley S, Schenk H, Karl M, Pforte A (2016) MR imaging of lung parenchymal changes in sarcoidosis. In: 13 imaging. European Respiratory Society, p PA3820
13. Rodríguez LR, Mejía C, Mallada BE, Prieto A, Mesa AA NEOE. Typical and atypical findings of pulmonary sarcoidosis at high resolution CT. In: ECR 2013. https://doi.org/10.1594/ecr2013/C-0169
14. Gümüştaş S, İnan N, Sarisoy HT, Anik Y, Arslan A, Çiftçi E et al (2011) Malignant versus benign mediastinal lesions: quantitative assessment with diffusion weighted MR imaging. Eur Radiol 21(11):2255–2260
15. Santos FS, Verma N, Marchiori E, Watte G, Medeiros TM, Mohammed TH, Hochhegger B (2021) MRI-based differentiation between lymphoma and sarcoidosis in mediastinal lymph nodes. J Bras Pneumol 47(2):e20200055
16. Abdel Razek AAK (2012) Diffusion magnetic resonance imaging of chest tumors. Cancer Imaging 12(3):452–463
17. Wang J, Takashima S, Takayama F et al (2001) Head and neck lesions: characterization with diffusion-weighted echo-planar MR imaging. Radiology 220(3):621–630

Publisher's Note
Springer Nature remains neutral with regard to jurisdictional claims in published maps and institutional affiliations.